AJNR

Comparing vascular morphology and hemodynamics in patients with vein of Galen malformations using intracranial 4D flow MRI

Jeffrey N. Stout, Alfred Pokmeng See, Julie Meadows, Shivani D. Rangwala and Darren B. Orbach

AJNR Am J Neuroradiol published online 24 May 2024
http://www.ajnr.org/content/early/2024/05/24/ajnr.A8353

Published May 24, 2024 as 10.3174/ajnr.A8353

ORIGINAL RESEARCH

Comparing vascular morphology and hemodynamics in patients with vein of Galen malformations using intracranial 4D flow MRI

Jeffrey N. Stout, Alfred Pokmeng See, Julie Meadows, Shivani D. Rangwala, and Darren B. Orbach

ABSTRACT

BACKGROUND AND PURPOSE: Vein of Galen malformation (VOGM) is the most common congenital cerebrovascular malformation, and many patients suffer high mortality rates and poor cognitive outcomes. Quantitative diagnostic tools are needed to improve clinical outcomes.

MATERIALS AND METHODS: A prospective study of children with VOGM was conducted by acquiring 4D flow MRI to quantify total blood inflow to the brain, flow in the pathologic falcine sinus, and flow in the superior sagittal sinus. Linear regression was used to test the relationships between these flows and age, clinical status, and the mediolateral diameter of the lesion's outflow tract through the falcine or straight sinus (MD), which is a known morphological prognostic metric.

RESULTS: In all 11 subjects (mean age 22±17 weeks [SD]), total blood flow to the brain always exceeded normal levels (1063±403 ml/min [mean±SD]). Significant correlations were observed between falcine sinus flow and MD, the posterior/middle cerebral artery flow ratio and age at scan, and between superior sagittal sinus flow proximal to malformation inflow and age at scan.

CONCLUSIONS: Using 4D flow MRI we established the hemodynamic underpinnings of MD, and investigated metrics representing parenchymal venous drainage that could be used to monitor the normalization of hemodynamics during embolization therapy.

ABBREVIATIONS: ACA = anterior cerebral artery; BA = basilar artery; MD = falcine or straight sinus mediolateral diameter; NAR = neonatal at risk; PCA = posterior cerebral artery; PCom = posterior communicating artery; SSS = superior sagittal sinus; VOGM = vein of Galen malformation.

Received month day, year; accepted after revision month day, year.
From the Cerebrovascular Surgery and Interventions Center, Boston Children's Hospital, Boston, MA, USA (J.N.S., A.P.S., J.M., D.B.O), and the Department of Neurosurgery, Keck School of Medicine, University of Southern California, Los Angeles, CA, USA (S.D.R.).

The authors declare no conflicts of interest related to the content of this article.

Please address correspondence to Jeffrey N Stout, PhD Cerebrovascular Surgery and Interventions Center, 300 Longwood Ave, Boston Children's Hospital, Boston, MA, USA, 02115, USA. jeffrey.stout@childrens.harvard.edu.

SUMMARY SECTION

PREVIOUS LITERATURE: A purely morphological marker of aggressive early clinical course, the mediolateral diameter of the falcine sinus, was established without corresponding hemodynamic observations. Separately, cerebral hemodynamic measurements in patients with vein of Galen malformation using 4D flow MRI have been reported in 2 studies. For 10 patients total, changes during serial embolization therapy included: inflow decreased, shunt flow decreased, and normal cerebral flow distribution established. A new MRI sequence with dual velocity encoding and kt-sense acceleration now permits whole slab flow measurements with a 1 mm^3 resolution in under 8 min.

KEY FINDINGS: In 11 subjects (mean age 22 **weeks**), total blood flow to the brain always exceeded normal levels. Significant correlations were observed between falcine sinus flow and i**ts** mediolateral diameter, the posterior/middle cerebral artery flow ratio and age at scan, and between superior sagittal sinus flow and age at scan.

KNOWLEDGE ADVANCEMENT: The hemodynamic underpinnings of the mediolateral diameter marker of aggressive clinical course were explicitly established. In addition, the flow through the superior sagittal sinus was identified as a possible marker of parenchymal venous drainage that may normalize after embolization therapy.

INTRODUCTION

Vein of Galen malformation (VOGM), a high flow intracranial arteriovenous shunt between the choroidal arteries and the prosencephalic vein of Markowski (Figure 1),[1] presents in neonates or young infants as high output cardiac failure with neurological comorbidities.[1,2] Endovascular treatment strategies developed in the 1980s and 1990s have provided therapeutic options for an otherwise fatal malformation,[3,4] but outcomes when VOGM is diagnosed fetally remain poor, with 1/3 not surviving past one year of age and another 1/3 suffering severe neurocognitive effects,[5] highlighting the necessity of further improvements to clinical care for these children.

The development of clear prognostic indicators for the neonatal course of the disease and eventual neurological outcomes would almost certainly be helpful in this regard.[6] A recent effort to identify prognosticators based on fetal imaging found that the mediolateral diameter

Copyright 2024 by American Society of Neuroradiology.

of the straight or falcine sinus at its narrowest point (MD) (Figure 1 B) was highly predictive of which neonates would have an aggressive early clinical course and require urgent embolizations after birth to control cardiopulmonary failure (i.e. the neonatal at risk cohort, NAR).[7] This anatomical metric was sufficiently accurate to decide which fetuses are eligible for a clinical trial of in-utero embolization for VOGM fetuses at high risk for brain injury or death.[8]

Another improvement would be the development of robust and reliable metrics of cerebral hemodynamics that could inform detailed planning of embolization therapy. Treatment planning is typically based on many factors,[2] but methods for observing individual cerebral hemodynamics and responses to embolization would give vast insight into the mechanisms of effective therapy.

4D flow MRI seems ideal for monitoring intracranial hemodynamics in VOGM. Accelerated 4D flow MRI provides sufficient resolution to accurately estimate flows through vessels in the circle of Willis as well as in draining venous structures.[9–11] Previous studies of a small number of patients with VOGM (N = 10, across two studies[12,13]) using 4D flow MRI have demonstrated complex hemodynamic changes with successive embolization procedures,[12–14] but work remains to develop these hemodynamic observations as useful prognosticators that might guide clinical management.

We observed intracranial blood flow dynamics using both 4D and 2D flow MRI to develop clinically useful flow-based indicators of risk and progression. We related our hemodynamic observations to MD in order to further support the clinical use of this biomarker, hypothesizing a strong correlation between flow and MD in the falcine sinus, and investigated several candidate metrics of parenchymal (i.e. non-lesional) blood flow which could be developed into biomarkers of response to therapy.

MATERIALS AND METHODS

Subsection Header

This prospective observational study was conducted with Institutional Review Board approval. From November 2021 to April 2023, all parents of children with VOGM who were referred to our hospital for evaluation and treatment of VOGM were approached to consent for 10-15 minutes of additional research scanning to be added at the end of their clinically indicated MRI studies. We have previously demonstrated that in the setting of VOGM, once parenchymal brain injuries begin to accrue there is nearly inevitable cascading effect whereby further injuries continue to develop, leaving patients at high risk of severe neurocognitive impairment.[15] As such, any infant with parenchymal injury severe enough to impact flow would be under a palliative care paradigm and therefore systematically excluded from clinical and research imaging. Patients underwent MRI scans according to clinical need and we added research imaging whenever feasible, as determined by researcher availability, scanner and patient schedules. This meant there was no research control over scan timing in relation to clinical events, as we collected data as opportunities presented themselves. During sedated scans to minimize motion, 4D flow imaging was attempted on 3T Siemens (Erlangen, Germany) Prisma and Skyra scanners where the sequence was available.

Patients were classified as NAR on the basis of severe cardiopulmonary distress at birth necessitating intubation and embolization therapy in the first 14 days of life. This was in contrast to stable, non-NAR neonates, who were discharged home to await their first embolization treatment around 6 months of age.

During the research portion of the scan, 4D and 2D flow imaging was collected. 4D flow MRI was used to measure hemodynamics in the Circle of Willis, the varix and the falcine sinus (repetition time (TR) = 82.6-92.8 ms, echo time (TE) = 3-3.2 ms, resolution = 0.8-1 mm isotropic, field-of-view (FOV) = 220 mm, k-t R = 5, 5 cardiac phases). Single and dual encoding velocity (VENC) 4D flow imaging was used depending on available imaging time with dual VENCs low= 60-80 cm/s, high = 100-160 cm/s and single VENCs=150 cm/s. VENCs were adjusted from default low/high = 80/160 cm/s when scout imaging or prior catheter angiography was available. 2D flow imaging (2D phase-contrast MRI) was used to measure the flow in the superior sagittal sinus (SSS) upstream from its junction with the falcine sinus (with the SSS at this location representing parenchymal brain drainage rather than malformation drainage), a location typically outside the feasible 4D flow imaging slab due to scan time constraints (Figure 1A) (TR = 65.76 ms, TE = 5.02 ms, resolution = 0.8 x 0.8 x 4 mm^3, FOV = 240 mm, VENC = 25-100 cm/s through plane, 10 cardiac phases).

Individual vessel flows were quantified. 4D flow data was corrected for Maxwell terms during reconstruction, and for eddy currents and velocity noise.[16,17] Vessel-wise flows were then calculated in a semi-automated fashion using a Matlab-based tool.[18] All automatic regions of interest along the vessels were manually reviewed for quality, excluding individual cut planes where the vessel size was transiently greater than 20% larger or smaller or was drawn on the incorrect adjacent vessel. SSS flows were quantified through manually defined vessel regions of interest drawn in Segment,[19] correcting for eddy currents.

Individual vessel flows were combined in various ways to check measurement quality and to investigate metrics of normal parenchymal inflow. Inflow conservation error, a previously developed data quality metric, was calculated as $|Q_{ICA}-Q_{ACA}-Q_{MCA}-Q_{PCOM}|/Q_{ICA}$.[11] There are various possible ways to quantify inflowing blood destined for parenchymal perfusion. In each metric we looked for normalization after therapy and evidence of the increase in cerebral blood flow over the first year of life. One metric would be non-shunting inflow, the difference between total inflow and falcine sinus flow. The quality of this metric would depend on the extent to which falcine flow represents shunt flow versus normal parenchymal drainage, but based on the pathophysiology of VOGM, the expectation would be that falcine sinus flow would be overwhelmingly lesional. A previous study found that MCA and PCA flows, in particular the PCA/MCA flow ratio indicated improved parenchymal perfusion after embolization.[12] The PCA:MCA flow ratio was calculated from the PCA and MCA vessel flows for each side. Inflow was the sum of ICA and BA flow. MD was measured following the previously described protocol.[7]

We created regression models using the Python-based statsmodels library including either a linear effect for MD (β_{MD}) or age at scan (β_{age}), and fixed effects for embolization status (α_{embo}) and NAR classification (α_{NAR}), to test relationships between these variables and inflow, non-shunting inflow, PCA:MCA flow ratio, individual vessel flows, and the fourth root of falcine flow. The fourth root of flow was a plausible transform following the intuition of Poiseuille's Law for pipes of approximately circular cross-section, which states flow is proportional to the fourth power of the radius.[20] Model residuals were tested for normality using the Shapiro-Wilk test with a level of $\alpha = 0.05$, and response variables transformed and regressions reanalyzed in cases where normality was not achieved, but there was an observed significant regression. P-values less than 0.05 were judged significant regressions. Analysis code can be found at

https://github.com/dittothat/vogm_4dflow.

RESULTS

The recruitment and exclusion flow diagram for all subjects is shown in Figure 2. All approached families consented to scanning, but some subjects underwent their subsequent clinical scan on a scanner without the 4D flow sequence installed, or at a time when research staff were unavailable. One subject underwent unsedated follow-up clinical scanning and was excluded from further analysis given known effects of sedation on cerebral blood flow precluding comparison with prior sedated scans.[21,22] Age and relevant clinical history of the subjects who underwent 4D flow imaging (N =11) are given in Table 1.

All 15 MRI flow measurements are provided in Supplemental Table 1. SSS measurements were not obtained for Subjects 2, 4 and 11 due to scanner schedule constraints. PCA measurements for Subject 3 were not possible using the automatic vessel segmentation algorithm. The right ACA for Subject 8 was too small to resolve. **Online Supplemental Data** contains the significant regression model fit results, and the results from all tested models are provided in Supplemental Table 2.

Inflow vessels

Inflow results are summarized in Figure 3. Data quality was generally acceptable with an average inflow conservation error of 24% (Supplemental Table 1). Total inflows were high, with no correlation to age (Figure 3 A).[23,24] In the three patients with serial observations, inflow always decreased after embolization. The high subject-wise variance in inflow masked the effect of embolization across the entire cohort (Supplemental Table 2).

We did not observe a significant correlation between non-shunting inflow and age at scan, nor a consistent change after embolization (Figure 3 B). The decrease for Subject 3 happens to correspond to a marked increase in flow conservation error, which hampers interpretation.

We did not observe significant correlations between age and PCA or MCA flows (Figure 3 C, D), although there was a significant negative correlation between the PCA/MCA flow ratio and age at scan (Figure 3 E, F). In addition, and clearly recognizing that our sample size was very small with serial results only for N = 2 subjects, we did not observe any significant trends between the PCA/MCA flow ratio and the time after embolization nor a resolution to the previously observed ratio of 0.55.[12]

Outflow vessels

Outflow results are summarized in Figure 4. Falcine sinus flow demonstrated a significant relationship with the modeled linear effect of MD (Figure 4 B), but the higher flow observations for Subjects 6 and 8 meant that the model residuals were not normally distributed (Figure 4 B). The modeled linear relationship between the fourth root of falcine sinus and MD was both significantly correlated and yielded residuals that were normally distributed (Figure 4 C). Furthermore, after subsequent embolization procedures, Subjects 2 and 3 appeared to have a flow to MD ratio that remained approximately constant, matching the observed cohort trend (Figure 4 A).

The final metric we considered related to parenchymal perfusion was SSS flow. There was a significant correlation between pre-falcine SSS flow and age, although all SSS flows were lower than what would be expected in this age range (Figure 4 D).[25] Subject 9 had an average retrograde SSS flow.

DISCUSSION

New MRI tools for flow quantification permit detailed observations of intracranial hemodynamics in VOGM. 4D flow MRI is a powerful modality for the simultaneous quantification of inflow and outflow vessels. We collected 4D flow data from 11 patients (previously only two studies of 10 patients total have presented 4D flow observations of patients with this disease, and only 5 were as young as our cohort), observing high brain blood inflow and a strong correlation between the fourth root of falcine sinus flow and MD, the previously described biomarker for NAR.[7] Additionally we explored metrics of parenchymal venous outflow, finding SSS flow anterior to the falcine sinus junction had a significant correlation with age, as expected.

High brain blood inflow has been previously observed in VOGM patients and reflects shunt flow. Quantitative inflow results have only been published for a total of 5 patients in the age range of our cohort (300-1800 ml/min),[12,13] with results similar to our observed range (570-2050 ml/min). Average inflow reduction of 40% from baseline to endpoint embolization was observed in a previous study,[12] and Subject 2 in our study had a 54% reduction in inflow (Figure 3 A).

The observed strong correlation between the fourth root of falcine flow and MD (Figure 1 B) significantly supports the use of MD as a structural biomarker of pathologic flow in the VOGM. Prior literature investigated only pretreatment MD and the likelihood of needing urgent neonatal treatment which was related to a more aggressive early clinical course that was assumed to be related to a greater lesional flow in these cases,[7] whereas flow observations can establish the link between the structure, pathophysiology, and clinical presentation.. Our study has proved that falcine sinus flow is related to MD, even in the post-natal and the post-treatment settings, based on the significant relationships between flow and MD even when controlling for embolization status **(Online Supplemental Data)**. Some subjects exhibited falcine sinus flow much higher than the modeled trend for flow versus MD (i.e. Subjects 6 and 9 in Supplemental Figure S1). We contend these subjects demonstrate the large range of intracranial hemodynamics in VOGM, and that more observations are needed to understand the nuances in the flow-morphology relationship for this lesion. This relationship is complex, because the craniocaudal diameter of the falcine sinus tends to be fixed, and so a smaller MD is an elliptical cylinder and a larger MD approaches a circular cylinder, which is different than comparing a flow through cylinders of different radii, where Poiseuille's law would completely explain the proportionality. Longitudinal measurements (Subjects 2 and 3) after subsequent embolizations corroborate a sustained relationship.

We sought a marker of the blood flow supplying parenchymal perfusion, that is, the non-arteriovenous shunt flow. Relying on the

knowledge that cerebral blood flow increases dramatically in the first year of life,[23,24] we looked for correlations between our candidate metrics and age and also expected normalization after embolization. We did not find these expected characteristics for non-shunting inflow, the inflow-falcine flow difference. This was puzzling, but may be due to the fact that inflow and falcine flow are highly related. Embolizations aim to increase the resistance of the shunt flow path, and this change causes both a reduction in inflow and, presumably, flow redistribution in the various normal drainage pathways of the brain, including through the internal cerebral veins, thefalcine sinus, and the SSS. Indeed, normal drainage through the internal cerebral veins is a known risk factor for hemorrhage after endovascular treatment.[26] This complex interaction between inflow and flow through the falcine sinus varies for each subject and at each timepoint. Indeed, approximating the non-shunting inflow metric from a past study, suggests no clear trends were revealed there either.[12] Thus, we reject non-shunting inflow as a useful metric reflecting parenchymal perfusion. In two subjects with serial embolizations, we did not observe a normalization in the PCA:MCA ratio (Figure G, H) as was previously observed,[12] but the ratio did decrease with age (**Online Supplemental Data** and Figure 3 E, F). The arterial flow to normal brain may be altered via arterial steal phenomenon or may not match age-expected levels if brain injury occurs from VOGM. Normalization of arterial brain inflow may occur over a variable extended time frame after exclusion of lesional flow by embolization, and if so, would not be reflected in our acute post-treatment imaging. SSS flow, anterior to the junction with the falcine sinus, showed a significant correlation with age (Figure 4 D). Our subjects all have lower SSS flow than the reference range (from limited previous observations[25]), and we hypothesize that this may reflect some degree of pressurization of the entire SSS by dint of the arterialized shunt inflow. Subject 3 did have higher SSS flow after embolization, but the final flow was still much lower than expected and in general we did not observe a significant resolution after embolization.

This study had a number of limitations. The research scan time allowed under general anesthesia, <15 minutes, impacted obtainable image resolution and coverage. Ideally we would position a thicker slab that would include the SSS locations we targeted with 2D flow MRI, but this was often out of reach within our designated scan time. The specific implementation of 4D flow MRI used in this study has been previously validated at another institution using flow phantoms.[11] Our average inflow conservation error of 24% is in line with expected flow conservation error when <3 voxels span the vessel lumen,[11] which is often the case for the ACA, MCA and PCA vessels in our subjects. As we collect data from more subjects, we will have the opportunity to set a rejection threshold based on this inflow conservation quality metric. Additionally, more subjects would support an investigation of non-linear relationships between flow, morphology and clinical parameters. Previous work classified NAR in ⅔ of the imaging cohort, consistent with previous reports,[7] so our sample is likely not representative of the full pathophysiological variety of VOGM. A larger, longer study of flow normalization is warranted. We only obtained follow up measurements for 3 subjects and only two had baseline, pre-treatment measurements. Our maximum follow-up duration was <8 months. Finally, more studies of cerebral blood flow in neonates are needed to establish reference ranges for this early period of development.[23–25] While several documented factors affect flow quantification accuracy,[11,24] we contend that 4D flow MRI would be ideal for the goal of establishing reference ranges of inflow and outflow vessels at young ages. However, it is known that anesthesia and sedation drive cerebral blood flow to be lower on average, though individual response varies (-50% to +20%).[21,22] It will be challenging to collect control flow values for anesthesia and sedation states matching our patient cohort in healthy children.

Next steps toward the development of hemodynamic metrics to guide prognosis and embolization therapy include exploring the flow and pressure relationships in the draining veins and collecting more observations from NAR patients. Additionally, the demonstration of a consistent relationship between flow and MD supports the measurement of MD to follow the physiologic status of patients who are not near advanced MR centers.

CONCLUSIONS

The observed correlation between falcine sinus flow and morphology, and the exploration of metrics of parenchymal flow finding SSS flow as significantly correlated with age, suggests the importance of venous outflow quantification to pathophysiology of VOGM. The simultaneous observation of flow across multiple vessels demonstrates the utility of 4D flow MRI for prognostication and guidance of therapy for patients with VOGM.

Table 1: Subjects who underwent sedated 4D flow MRI.

Subject ID	Age at first scan (weeks)	History at time of first scan	Neonatal at risk	# of scans
1	61.2	s/p angiogram (no embolization)	0	1
2	23.8	no previous interventions	0	3
3	11.1	s/p embolization 1 day previously	0	2
4	24.0	s/p embolization same day	0	1
5	16.9	s/p embolization same day	0	1
6	0.1	no interventions, later deceased	1	1
7	0.9	s/p embolization 2 days previously	1	1
8	20.9	no interventions, coarctation of the aorta	0	1
9	19.4	no previous interventions	0	1
10	36.7	no previous interventions	0	1
11	26.7	no previous interventions	0	2
	Avg = 22		N = 2	N = 15

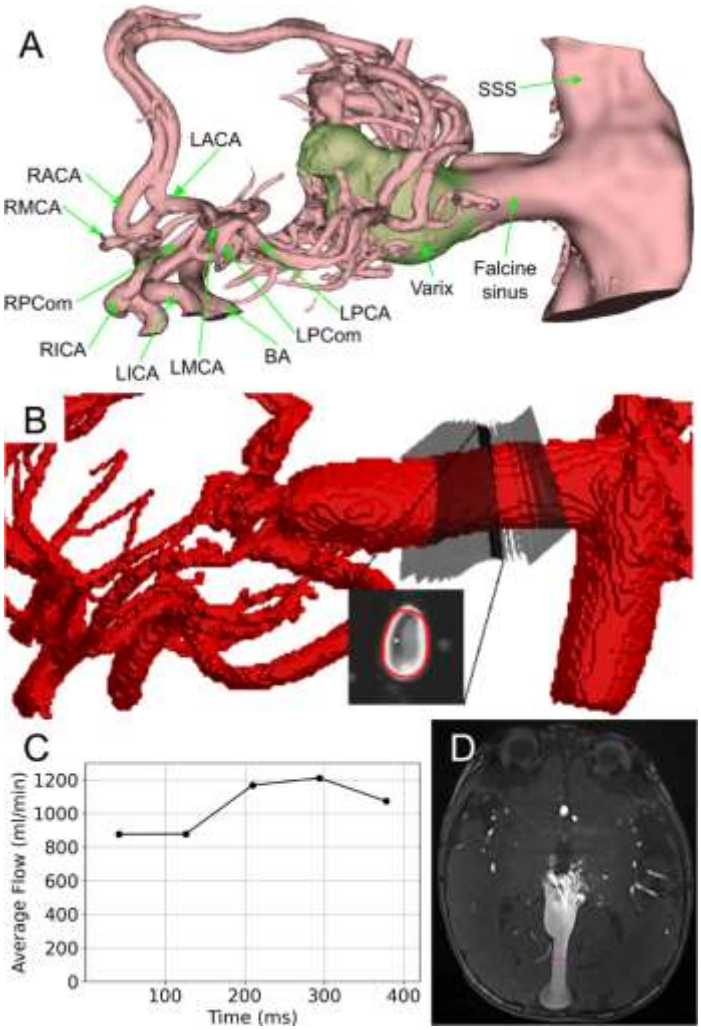

FIG 1. (A) Example vascular anatomy in VOGM. The complex plexiform nexus draining into the varix originates from segments of the posterior choroidal and anterior cerebral arteries. For the first scan of Subject 2, (B) example 4D-flow automated cut plane and ROI extraction for the falcine sinus segment, (C) time resolved flow averaged across all cut planes, and (D) mediolateral diameter measurement based on time-of-flight MR angiogram. Vessel abbreviations are: anterior cerebral artery (ACA), basilar artery (BA), internal carotid artery (ICA), middle cerebral artery (MCA), posterior cerebral artery (PCA), posterior communicating artery (PCOM), and superior sagittal sinus (SSS).

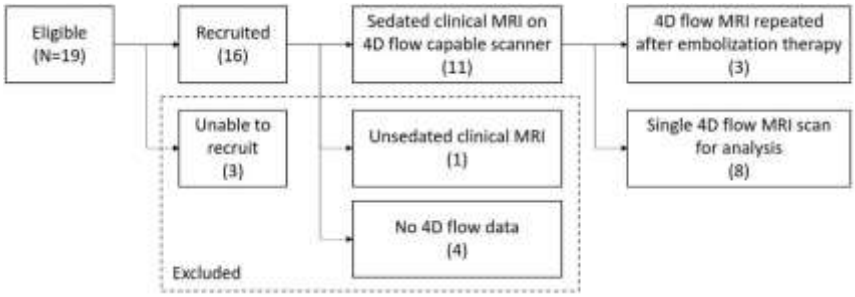

FIG 2. Flow diagram of subjects in this study.

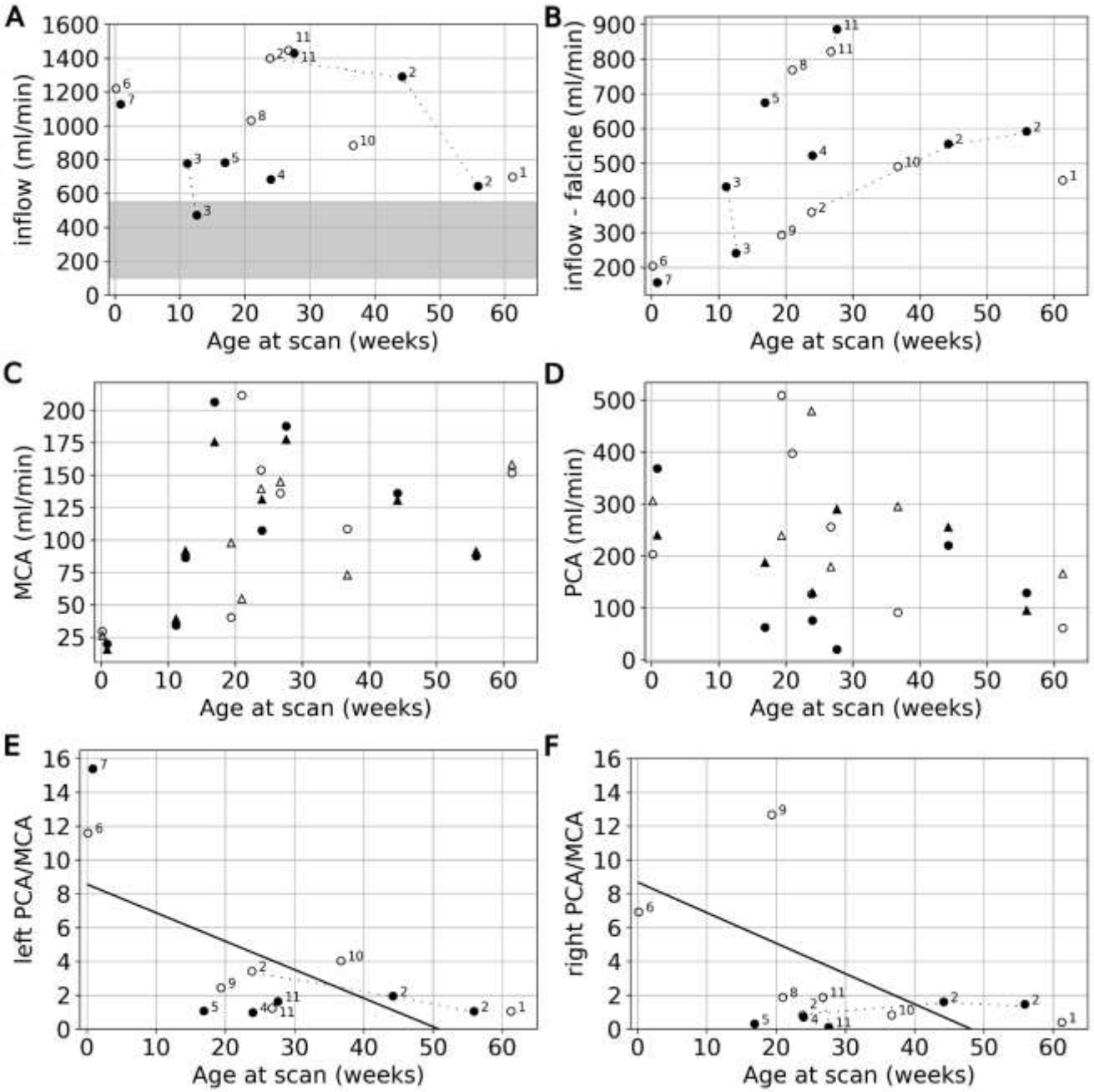

FIG 3. Quantitative inflow results from 4D flow MRI with pre-embolization open markers, post-embolization closed markers, and subsequent measurements connected by dotted lines. Labels indicate subject number. (A) Total inflow through the ICAs and BA versus age, with the normal range of blood flow in this age range indicated by the gray shading.22,23 (B) Non-shunting inflow (inflow-falcine flow) versus age, no significant correlation. (C, D) MCA and PCA flow versus age, right side are circles, and left side are triangles, no significant correlation. (E, F) The PCA/MCA ratio versus age at scan was significantly correlated on both the left (P=0.015) and the right (P=0.038).

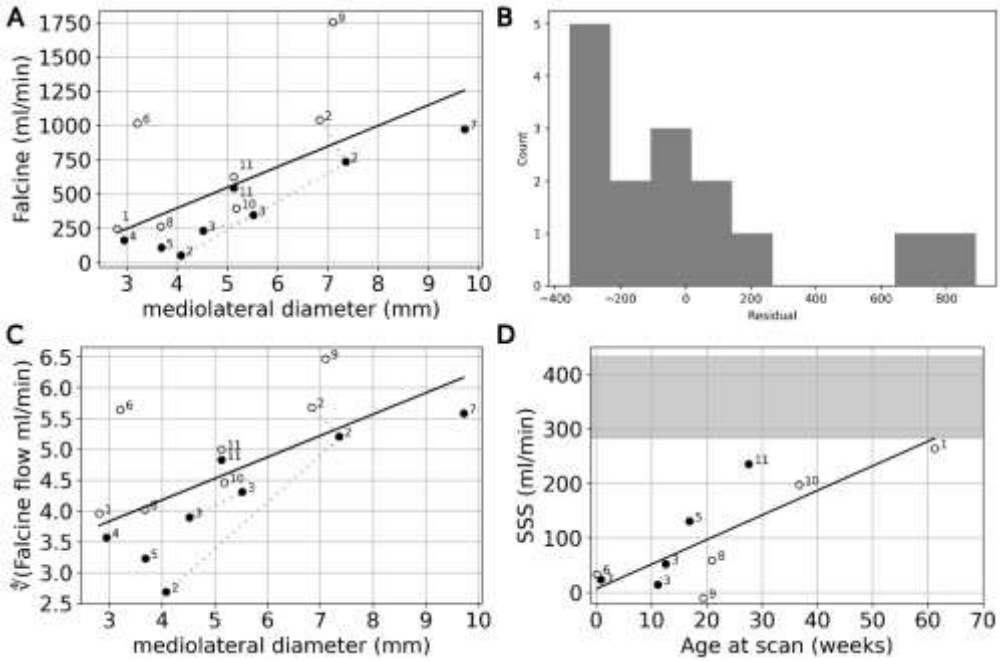

FIG 4 Quantitative outflow results from 4D flow MRI for the falcine sinus and 2D Flow MRI for the SSS. (A) Falcine sinus flow versus MD was significantly correlated (151 [37, 264] (slope [95% CI]), P=0.013). (B) The histogram of the residuals of the model of Falcine sinus flow versus MD are not normally distributed (Shapiro wilks W=0.79, P=0.003). (C) The fourth root of Falcine sinus flow versus MD was significantly correlated with MD (0.35 [0.10, 0.59], P=0.009). (D) 2D flow MRI results from the SSS pre-falcine inflow were correlated with age at scan (4.51 [1.92, 7.10], P=0.004) with normal range of SSS blood flow from 29-60 weeks indicated by the gray shading.[25]

ACKNOWLEDGMENTS

Funding for this study was from the Sage Schermerhorn Chair in Image-Guided Therapy. Thanks to Maria Aristova for providing the Matlab tools and training to process the data that were collected using the 4D flow sequence developed by Sussanne Schnell.

REFERENCES

1. Raybaud CA, Strother CM, Hald JK. Aneurysms of the vein of Galen: embryonic considerations and anatomical features relating to the pathogenesis of the malformation. *Neuroradiology* 1989;31:109–28.

2. Cordova EG, Levy P, Kheir JN, et al. Vein of Galen Malformation. *Neoreviews* 2020;21:e678–86.

3. Lasjaunias P, Garcia-Monaco R, Rodesch G, et al. Vein of Galen malformation - Endovascular management of 43 cases. *Childs Nerv Syst* 1991;7:360–7.

4. Lasjaunias PL, Chng SM, Sachet M, et al. The management of vein of Galen aneurysmal malformations. *Neurosurgery* 2006;59:184–94.

5. D'Amico A, Tinari S, D'Antonio F, et al. Outcome of fetal Vein Galen aneurysmal malformations: a systematic review and meta-analysis. *J Matern Fetal Neonatal Med* 2022;35:5312–7.

6. Paladini D, Deloison B, Rossi A, et al. Vein of Galen aneurysmal malformation (VGAM) in the fetus: retrospective analysis of perinatal prognostic indicators in a two-center series of 49 cases. *Ultrasound Obstet Gynecol* 2017;50:192–9.

7. Arko L, Lambrych M, Montaser A, et al. Fetal and Neonatal MRI Predictors of Aggressive Early Clinical Course in Vein of Galen Malformation. *AJNR Am J Neuroradiol* 2020;41:1105–11.

8. Orbach DB, Wilkins-Haug LE, Benson CB, et al. Transuterine Ultrasound-Guided Fetal Embolization of Vein of Galen Malformation, Eliminating Postnatal Pathophysiology. *Stroke* https://doi.org/10.1161/STROKEAHA.123.043421.

9. Schnell S, Ansari SA, Wu C, et al. Accelerated dual-venc 4D flow MRI for neurovascular applications. *J Magn Reson Imaging* 2017;46:102–14.

10. Schnell S, Wu C, Ansari SA. Four-dimensional MRI flow examinations in cerebral and extracerebral vessels - ready for clinical routine? *Curr Opin Neurol* 2016;29:419–28.

11. Aristova M, Vali A, Ansari SA, et al. Standardized Evaluation of Cerebral Arteriovenous Malformations Using Flow Distribution Network Graphs and Dual-venc 4D Flow MRI. *J Magn Reson Imaging* 2019;50:1718–30.

12. Wu C, Schoeneman SE, Kuhn R, et al. Complex Alterations of Intracranial 4-Dimensional Hemodynamics in Vein of Galen Aneurysmal Malformations During Staged Endovascular Embolization. *Oper Neurosurg (Hagerstown)* 2016;12:239–49.

13. Li Y, Ahmed R, Rivera-Rivera LA, et al. Serial Quantitative and Qualitative Measurements of Flow in Vein of Galen Malformations Using 4-Dimensional Flow Magnetic Resonance Imaging (Phase Contrast Vastly undersampled Isotropic PRojection). *World Neurosurg* 2019;126:405–12.

14. Hadad S, Rangwala SD, Stout JN, et al. Understanding development of jugular bulb stenosis in vein of galen malformations: identifying metrics of complex flow dynamics in the cerebral venous vasculature of infants. *Front Physiol* 2023;14:1113034.

15. Jaimes C, Machado-Rivas F, Chen K, et al. Brain injury in fetuses with vein of Galen malformation and nongalenic arteriovenous fistulas: Static snapshot or a portent of more? *AJNR Am J Neuroradiol* 2022;43:1036–41.

16. Bock J, Kreher BW, Hennig J, et al. Optimized pre-processing of time-resolved 2D and 3D phase contrast MRI data. In: *Proceedings of the 15th Annual meeting of ISMRM, Berlin, Germany.*; 2007:3138.

17. Bernstein MA, Zhou XJ, Polzin JA, et al. Concomitant gradient terms in phase contrast MR: analysis and correction. *Magn Reson Med* 1998;39:300–8.

18. Vali A, Aristova M, Vakil P, et al. Semi-automated analysis of 4D flow MRI to assess the hemodynamic impact of intracranial atherosclerotic disease. *Magn Reson Med* 2019;82:749–62.

19. Heiberg E, Sjögren J, Ugander M, et al. Design and validation of Segment--freely available software for cardiovascular image analysis. *BMC Med Imaging* 2010;10:1.

20. Lekner J. Viscous flow through pipes of various cross-sections. *Eur J Phys* 2007;28:521.

21. Lynch JM, Ko T, Newland JJ, et al. Effect of anesthesia on cerebral oxygenationand blood flow in neonates with critical congenital heart disease. In: *OSA Biomedical Optics Congress.*; 2016.

22. Slupe AM, Kirsch JR. Effects of anesthesia on cerebral blood flow, metabolism, and neuroprotection. *J Cereb Blood Flow Metab* 2018;38:2192–208.

23. Varela M, Groves AM, Arichi T, et al. Mean cerebral blood flow measurements using phase contrast MRI in the first year of life. *NMR Biomed* 2012;25:1063–72.

24. Liu P, Qi Y, Lin Z, et al. Assessment of cerebral blood flow in neonates and infants: A phase-contrast MRI study. *Neuroimage* 2019;185:926–33.

25. Wu C, Honarmand AR, Schnell S, et al. Age-related changes of normal cerebral and cardiac blood flow in children and adults aged 7 months to 61 years. *J Am Heart Assoc* 2016;5:1–14.

26. Bhatia K, Mendes Pereira V, Krings T, et al. Factors Contributing to Major Neurological Complications From Vein of Galen Malformation Embolization. *JAMA Neurol* 2020;77:992–9.

SUPPLEMENTAL FILES

Online Supplemental Data: Significant regression models. Flows (ml/min) were modeled as different linear combinations of age (weeks), MD, NAR and embolization, where NAR was the dummy variable 1 when present, and embolization was 1 when it had occurred prior to the MRI. Values presented as coefficient [95% confidence interval]. Bolded values indicate $P < 0.05$. See Supplemental Table 2 for all tested regression models.

Response variable	Intercept	β_{age}	β_{MD}	α_{NAR}	α_{embo}	N	Residual normality
Left PCA:MCA	**8.56 [4.30, 12.82] P=0.001**	**-0.17 [-0.30, -0.04] P=0.015**	-	-	-	12	W=0.94, P=0.541
Left PCA:MCA	**8.68 [3.51, 13.86] P=0.004**	**-0.17 [-0.30, -0.03] P=0.021**	-	-	-0.24 [-5.20, 4.71] P=0.913	12	W=0.93, P=0.432
Right PCA:MCA	**8.68 [3.16, 14.19] P=0.005**	**-0.18 [-0.35, -0.01] P=0.038**	-	-	-	13	W=0.88, P=0.063
Right PCA:MCA	**8.51 [2.05, 14.96] P=0.015**	**-0.18 [-0.36, -0.00] P=0.048**	-	-	0.40 [-5.91, 6.71] P=0.891	13	W=0.89, P=0.101
falcine	-206 [-823, 411] P=0.484	-	**151 [37, 264] P=0.013**	-	-	15	**W=0.79, P=0.003**
$\sqrt[4]{}$falcine	**2.79 [1.44, 4.13] P=0.001**	-	**0.35 [0.10, 0.59] P=0.009**	-	-	15	W=0.97, P=0.817
$\sqrt[4]{}$falcine	**3.16 [2.10, 4.21] P=0.000**	-	**0.39 [0.20, 0.58] P=0.001**	-	**-1.07 [-1.78, -0.36] P=0.007**	15	W=0.98, P=0.969
$\sqrt[4]{}$falcine	**3.22 [2.18, 4.27] P=0.000**	-	**0.36 [0.16, 0.55] P=0.002**	0.62 [-0.45, 1.68] P=0.227	**-1.04 [-1.75, -0.34] P=0.007**	15	W=0.97, P=0.849
SSS	6.70 [-62.97, 76.37] P=0.830	**4.51 [1.92, 7.10] P=0.004**	-	-	-	10	W=0.98, P=0.972
SSS	-33.58 [-131.62, 64.47] P=0.445	**5.15 [2.38, 7.91] P=0.003**	-	-	54.08 [-40.70, 148.86] P=0.219	10	W=0.96, P=0.758
SSS	-79.61 [-215.14, 55.92] P=0.201	**6.30 [2.67, 9.93] P=0.005**	-	70.17 [-72.07, 212.41] P=0.273	70.11 [-30.32, 170.54] P=0.138	10	W=0.89, P=0.172

Supplemental Table 1: Vessel-wise flow (ml/min), inflow conservation error, and mediolateral diameter measurements (mm). SSS flow values from 2D flow MRI.

Subject	Session	Age at Scan (weeks)	RICA	LICA	BA	RACA	RMCA	RPCOM	LACA	LMCA	LPCOM	RPCA	LPCA	SSS	Falcine	Inflow	Avg Inflow conservation error	MD
1	1	61.2	253	218	227	68	152	101	22	158	118	61	166	264	247	698	32%	2.8
2	1	23.8	409	469	523	261	154	118	269	140	97	127	479	NA	1042	1400	19%	6.8
2	2	44.2	373	453	466	92	136	170	82	131	143	220	256	NA	736	1291	14%	7.4
2	3	55.9	205	209	230	0	88	60	61	91	32	129	96	NA	52	644	20%	4.1
3	1	11.1	257	202	319	11	34	202	140	39	72	NA	NA	14	346	778	14%	5.5
3	2	12.6	132	108	232	0	86	122	92	92	42	NA	NA	53	231	471	83%	4.5
4	1	24.0	168	257	259	0	108	20	91	132	0	76	129	NA	162	684	19%	3.0
5	1	16.9	181	304	299	55	206	0	195	176	18	63	188	131	109	784	36%	3.7
6	1	0.1	388	415	418	68	29	256	107	26	170	203	306	34	1017	1221	18%	3.2
7	1	0.9	290	326	513	70	20	368	61	16	240	368	240	24	973	1129	30%	9.7
8	1	20.9	410	222	400	NA	212	196	67	55	61	397	NA	59	263	1032	9%	3.7
9	1	19.4	416	545	1086	142	40	241	98	98	107	509	239	-10	1754	2047	23%	7.1
10	1	36.7	289	220	376	24	109	184	43	73	35	91	296	197	395	885	21%	5.2
11	1	26.7	386	397	663	84	136	194	53	145	218	256	180	NA	625	1447	6%	5.1
11	2	27.6	408	421	602	115	188	193	50	178	245	20	290	236	545	1431	17%	5.1

Supplemental Table 2: All regression models. Flows (ml/min) were modeled as different linear combinations of age (weeks), MD, NAR and embolization, where NAR was the dummy variable 1 when present, and embolization was 1 when it had occurred prior to the MRI. Values presented as coefficient [95% confidence interval]. Bolded values indicate P < 0.05.

Response variable	Intercept	β_{age}	β_{MD}	α_{NAR}	α_{embo}	N	Residual normality
inflow	**1175 [752, 1599] P=0.000**	-4 [-18, 9] P=0.501	-	-	-	15	W=0.95, P=0.465
inflow	**1390 [912, 1867] P=0.000**	-5 [-18, 8] P=0.391	-	-	-361 [-807, 86] P=0.104	15	W=0.92, P=0.168
inflow	**1414 [785, 2044] P=0.000**	-6 [-23, 11] P=0.452	-	-55 [-896, 786] P=0.889	-363 [-836, 110] P=0.119	15	W=0.92, P=0.199
Left PCA:MCA	**8.56 [4.30, 12.82] P=0.001**	**-0.17 [-0.30, -0.04] P=0.015**	-	-	-	12	W=0.94, P=0.541
Left PCA:MCA	**8.68 [3.51, 13.86] P=0.004**	**-0.17 [-0.30, -0.03] P=0.021**	-	-	-0.24 [-5.20, 4.71] P=0.913	12	W=0.93, P=0.432
Right PCA:MCA	**8.68 [3.16, 14.19] P=0.005**	**-0.18 [-0.35, -0.01] P=0.038**	-	-	-	13	W=0.88, P=0.063
Right PCA:MCA	**8.51 [2.05, 14.96] P=0.015**	**-0.18 [-0.36, -0.00] P=0.048**	-	-	0.40 [-5.91, 6.71] P=0.891	13	W=0.89, P=0.101
RPCA	**287.65 [124.24, 451.06] P=0.003**	-3.40 [-8.40, 1.60] P=0.163	-	-	-	13	W=0.94, P=0.518
RPCA	**324.45 [142.91, 505.99] P=0.003**	-3.31 [-8.34, 1.72] P=0.173	-	-	-84.82 [-262.22, 92.58] P=0.312	13	**W=0.86, P=0.034**
LPCA	**291.84 [174.37, 409.31] P=0.000**	-1.89 [-5.40, 1.62] P=0.258	-	-	-	12	W=0.90, P=0.182
LPCA	**330.11 [201.06, 459.15] P=0.000**	-1.88 [-5.27, 1.52] P=0.243	-	-	-77.33 [-200.77, 46.11] P=0.190	12	W=0.89, P=0.121
RMCA	**77.60 [16.90, 138.31] P=0.016**	1.40 [-0.58, 3.37] P=0.150	-	-	-	15	W=0.90, P=0.092
RMCA	**81.60 [5.05, 158.14] P=0.039**	1.38 [-0.69, 3.46] P=0.173	-	-	-6.72 [-78.36, 64.91] P=0.841	15	W=0.90, P=0.108
LMCA	**64.85 [17.25, 112.45] P=0.011**	1.51 [-0.04, 3.06] P=0.056	-	-	-	15	W=0.92, P=0.191
LMCA	**57.91 [-1.70, 117.52] P=0.056**	1.54 [-0.08, 3.15] P=0.061	-	-	11.68 [-44.11, 67.47] P=0.656	15	W=0.95, P=0.528
non-shunting inflow	**369.16 [155.23, 583.08] P=0.003**	5.00 [-1.96, 11.96] P=0.144	-	-	-	15	**W=0.87, P=0.038**
non-shunting inflow	**346.57 [77.55, 615.58] P=0.016**	5.09 [-2.20, 12.39] P=0.154	-	-	38.01 [-213.75, 289.78] P=0.748	15	**W=0.86, P=0.026**
non-shunting inflow	**491.73 [175.11, 808.35] P=0.006**	1.42 [-6.96, 9.81] P=0.715	-	-323.04 [-746.14, 100.05] P=0.121	21.79 [-216.12, 259.69] P=0.844	15	W=0.95, P=0.489
falcine	**806 [355, 1257] P=0.002**	-9 [-24, 5] P=0.189	-	-	-	15	W=0.91, P=0.151
falcine	**1043 [540, 1546] P=0.001**	-10 [-24, 3] P=0.123	-	-	-399 [-869, 72] P=0.090	15	W=0.93, P=0.273
falcine	-206 [-823, 411] P=0.484	-	**151 [37, 264] P=0.013**	-	-	15	**W=0.79, P=0.003**
falcine	-49 [-562, 463] P=0.837	-	**168 [75, 260] P=0.002**	-	**-456 [-802, -110] P=0.014**	15	W=0.91, P=0.134
falcine	-23 [-545, 499] P=0.926	-	**155 [58, 252] P=0.005**	238 [-293, 769] P=0.345	**-446 [-796, -95] P=0.017**	15	W=0.94, P=0.379
$\sqrt[4]{}$falcine	**2.79 [1.44, 4.13] P=0.001**	-	**0.35 [0.10, 0.59] P=0.009**	-	-	15	W=0.97, P=0.817
$\sqrt[4]{}$falcine	**3.16 [2.10, 4.21] P=0.000**	-	**0.39 [0.20, 0.58] P=0.001**	-	**-1.07 [-1.78, -0.36] P=0.007**	15	W=0.98, P=0.969
$\sqrt[4]{}$falcine	**3.22 [2.18, 4.27] P=0.000**	-	**0.36 [0.16, 0.55] P=0.002**	0.62 [-0.45, 1.68] P=0.227	**-1.04 [-1.75, -0.34] P=0.007**	15	W=0.97, P=0.849
SSS	6.70 [-62.97, 76.37] P=0.830	**4.51 [1.92, 7.10] P=0.004**	-	-	-	10	W=0.98, P=0.972
SSS	-33.58 [-131.62, 64.47] P=0.445	**5.15 [2.38, 7.91] P=0.003**	-	-	54.08 [-40.70, 148.86] P=0.219	10	W=0.96, P=0.758
SSS	-79.61 [-215.14, 55.92] P=0.201	**6.30 [2.67, 9.93] P=0.005**	-	70.17 [-72.07, 212.41] P=0.273	70.11 [-30.32, 170.54] P=0.138	10	W=0.89, P=0.172

Supplemental Figure 1: The PCA/MCA ratio versus time after embolization on both sides. Results from 4D flow MRI with pre-embolization open markers, post-embolization closed markers, and subsequent measurements connected by dotted lines. Labels indicate subject number.